Обзор ArXiv/astro-ph, 7-11 декабря 2020

От Сильченко О.К.

ArXiv: 2012.05363

Revisiting the Integrated Star Formation Law. II. Starbursts and the Combined Global Schmidt Law

ROBERT C. KENNICUTT JR.[1,2,3] AND MITHI A. C. DE LOS REYES[4,3]

[1] *Department of Astronomy and Steward Observatory, University of Arizona*
Tucson, AZ 85721, USA

[2] *Department of Physics and Astronomy, Texas A&M University*
College Station, TX 77843, USA

[3] *Institute of Astronomy, University of Cambridge*
Madingley Road, Cambridge CB3 0HA, UK

[4] *Department of Astronomy, California Institute of Technology*
1200 E. California Blvd., MC 249-17
Pasadena, CA 91125, USA

Submitted to ApJ

ABSTRACT

We compile observations of molecular gas contents and infrared-based star formation rates (SFRs) for 112 circumnuclear star forming regions, in order to re-investigate the form of the disk-averaged Schmidt surface density star formation law in starbursts. We then combine these results with total gas and SFR surface densities for 153 nearby non-starbursting disk galaxies from de los Reyes & Kennicutt (2019), to investigate the properties of the combined star formation law, following Kennicutt (1998; K98). We confirm that the combined Schmidt law can be fitted with a single power law with slope $n = 1.5 \pm 0.05$ (including fitting method uncertainties), somewhat steeper than the value $n = 1.4 \pm 0.15$

Выборка из 112 ‘starbursts’ (LIRG+hot spots)

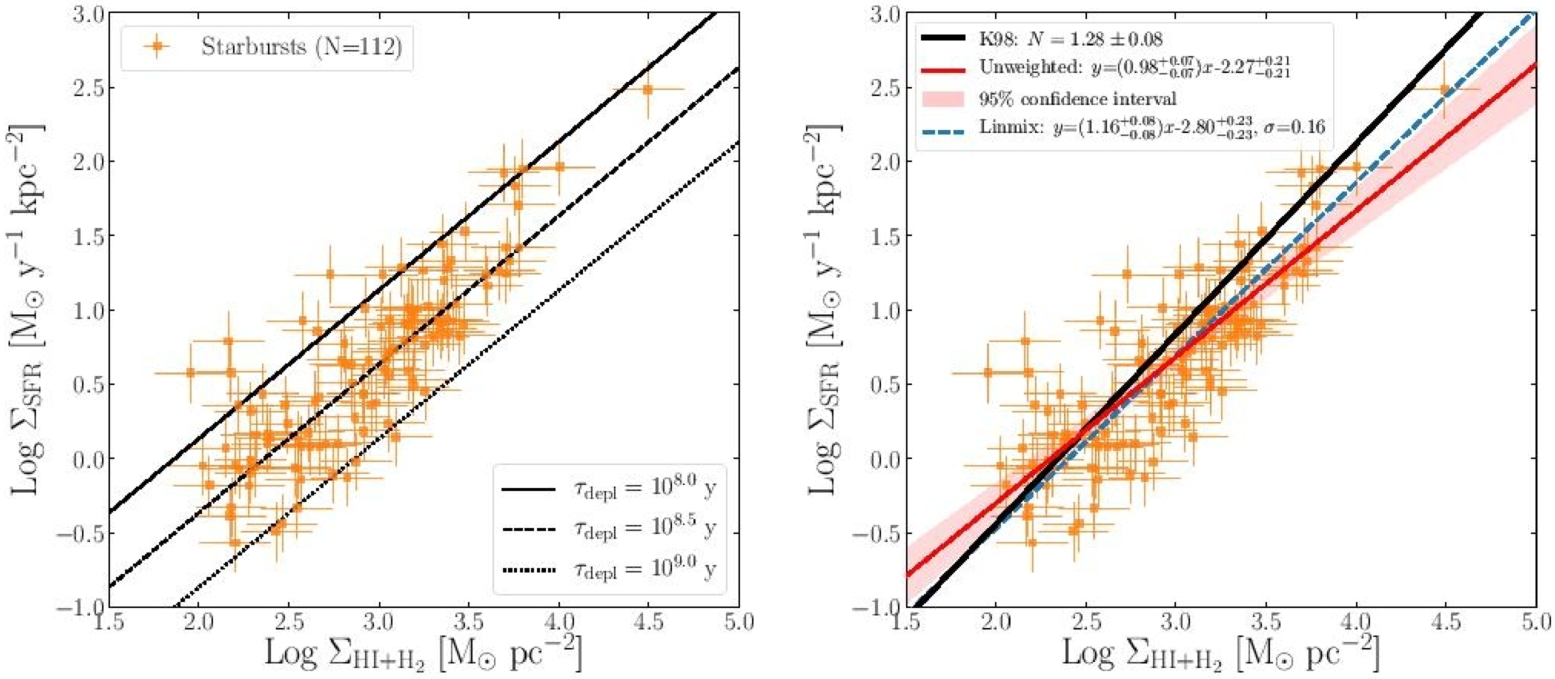

Figure 2. Schmidt law for the starburst galaxy sample. The left panel overlays lines of constant molecular gas depletion times, and the right panel overlays maximum likelihood fits to the starburst galaxy sample, and the fit derived previously for a smaller sample by K98 (solid black line), adjusted to consistent choices for the IMF and CO-to-H_2 conversion factor. All molecular surface densities were derived using a Milky Way value for X(CO). The starburst disks are all molecular dominated so the H_2 surface density is taken as proxy for the total gas surface density.

А если вместе с ‘нормальными’ спиралями?

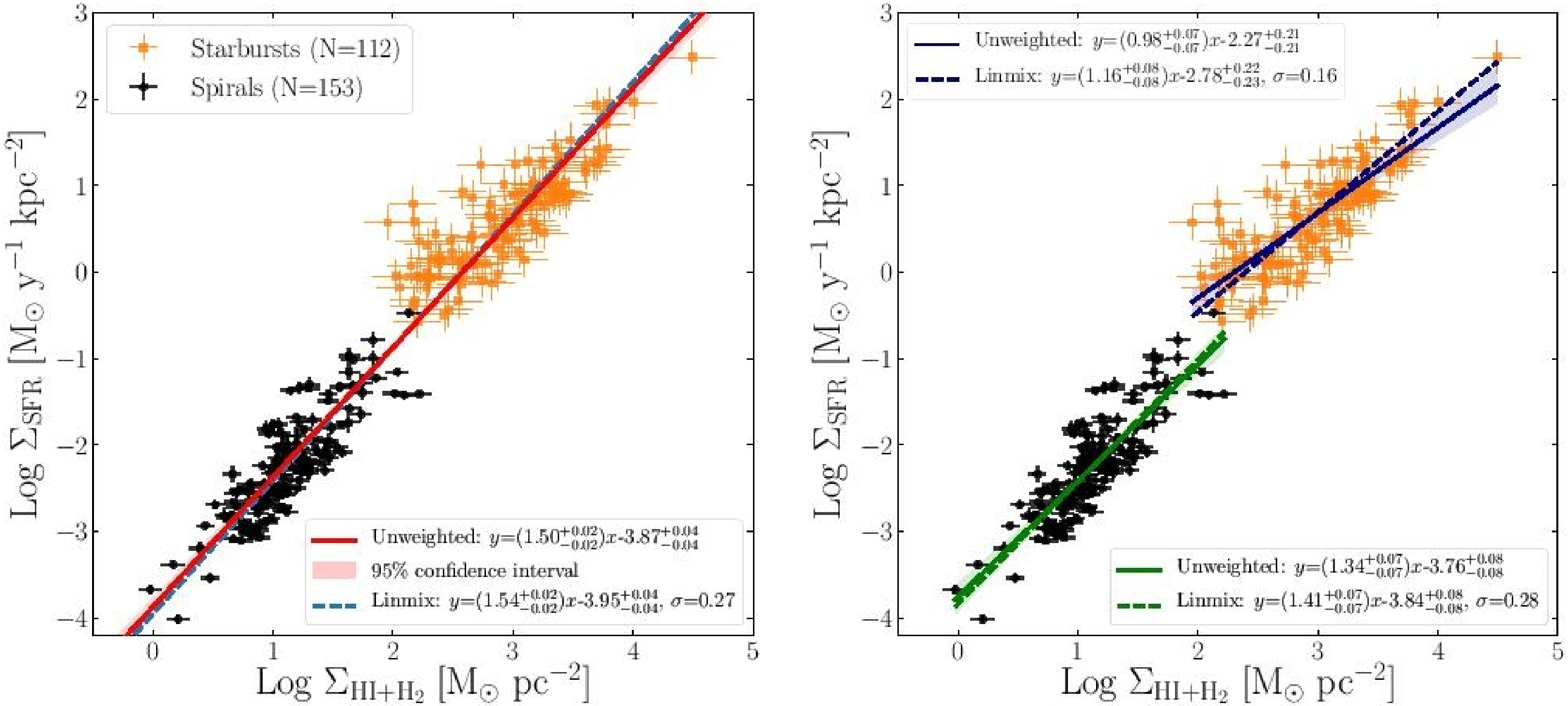

Figure 3. Relation between SFR surface density and total (atomic plus molecular) gas surface density for the the combined sample of normal spiral disks from Paper I (black points) and the starbursts in this sample (orange points). A constant Milky Way value for the CO-to-H_2 conversion factor is assumed for all galaxies. Left: A single power law is fitted to all of the data. Right: Separate power laws are fitted to the normal galaxies and the starburst galaxies. Shaded regions represent 95% confidence intervals about the unweighted fits.

Потому что разные времена исчерпания…

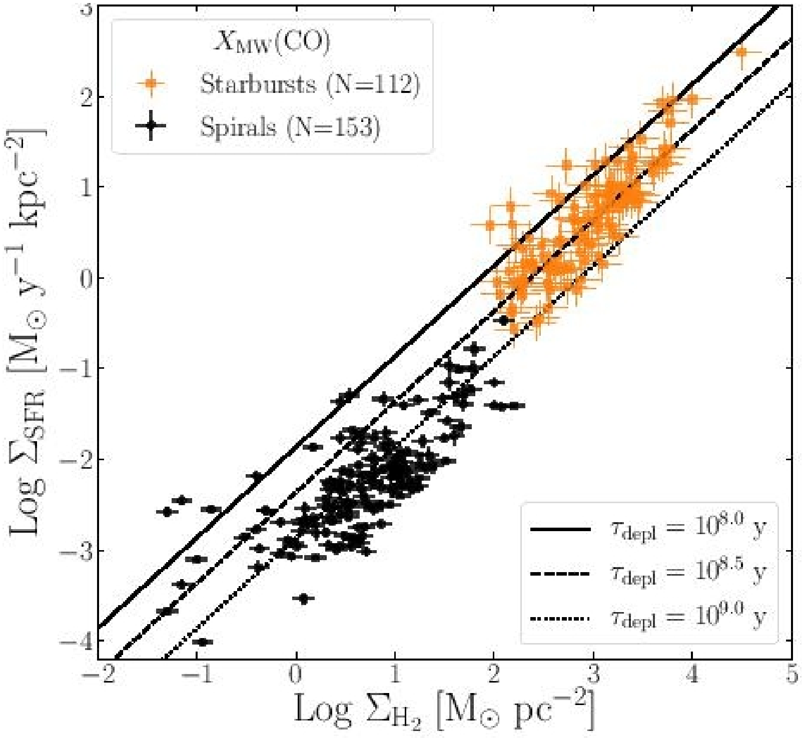

Figure 4. Relation between SFR surface density and molec-ular gas surface density for the the combined sample of nor-mal spiral disks from Paper I (black points) and the star-bursts in this sample (orange points). A constant Milky Way value for the CO-to-H_2 conversion factor is assumed for al galaxies. Lines represent constant molecular gas depletior times.

Динамика всех примиряет?

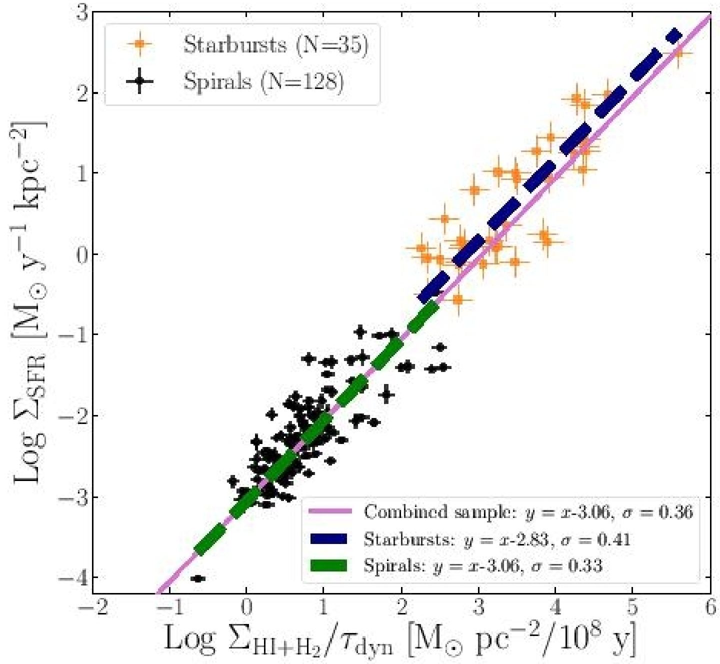

Figure 5. Correlation between SFR surface density and the ratio of total gas surface density to the orbital period at the outer edge of the star-forming disks, or "Silk-Elmegreen" law. Normal and starbursts are indicated as in Figure 3. The solid points assume a fixed (Milky Way) value of the X(CO) conversion factor for all galaxies. The pink solid line indicates the best-fit line with slope fixed to unity for the composite sample, while the blue and green dashed lines indicate the best-fit lines for the starburst and spiral samples, respectively. Root-mean-square dispersions are listed as σ.

ArXiv: 2012.04771

The ALMaQUEST Survey: V. The non-universality of kpc-scale star formation relations and the factors that drive them

Sara L. Ellison[1], Lihwai Lin[2], Mallory D. Thorp[1], Hsi-An Pan[3], Jillian M. Scudder[4], Sebastian F. Sánchez[5], Asa F. L. Bluck[6], Roberto Maiolino[6]

[1] *Department of Physics & Astronomy, University of Victoria, Finnerty Road, Victoria, British Columbia, V8P 1A1, Canada*
[2] *Institute of Astronomy & Astrophysics, Academia Sinica, Taipei 10617, Taiwan*
[3] *Max-Planck-Institut für Astronomie, Königstuhl 17, D-69117 Heidelberg, Germany*
[4] *Department of Physics and Astronomy, Oberlin College, Oberlin, Ohio, OH 44074, USA*
[5] *Instituto de Astronomía, Universidad Nacional Autonoma de Mexico, A. P. 70-264, C.P. 04510, Mexico, D.F., Mexico*
[6] *Kavli Institute for Cosmology & Cavendish Astrophysics, University of Cambridge, Madingley Road, Cambridge, CB3 0HA, UK*

10 December 2020

ABSTRACT

Using a sample of ~15,000 kpc-scale star-forming spaxels in 28 galaxies drawn from the ALMA-MaNGA QUEnching and STar formation (ALMaQUEST) survey, we investigate the galaxy-to-galaxy variation of the 'resolved' Schmidt-Kennicutt relation (rSK; Σ_{H_2} - Σ_{SFR}), the 'resolved' star forming main sequence (rSFMS; $\Sigma_{\star}$ - Σ_{SFR}) and the 'resolved' molecular gas main sequence (rMGMS; $\Sigma_{\star}$ - Σ_{H_2}). The rSK relation, rSFMS and rMGMS all show significant galaxy-to-galaxy variation in both shape and normalization, indicating that none of these relations is universal between galaxies. The rSFMS shows the largest galaxy-to-galaxy variation and the rMGMS the least. By defining an 'offset' from the average relations, we compute a ΔrSK, ΔrSFMS, ΔrMGMS for each galaxy, to investigate correlations with global properties. We find the following correlations with at least 2σ significance: the rSK is lower (i.e. lower star formation efficiency) in galaxies with higher $M_{\star}$, larger Sersic index and lower

MaNGa+ALMA: 28 галактик

Table 1. Summary of global properties for ALMaQUEST galaxies used in this work. The number of spaxels indicates the number in each galaxy that pass the various detection and S/N thresholds required in both CO and in optical emission lines.

Plate-ifu	z	$\log(M_\star/M_\odot)$	log (SFR/yr)	Sersic N_s	# spaxels
8241-3703	0.02911	10.11	0.25	1.5	555
8615-3703	0.01845	10.19	0.40	1.6	291
8084-3702	0.02206	10.23	0.43	1.5	167
8082-6103	0.02416	10.31	0.39	1.4	784
8952-6104	0.02843	10.33	0.46	2.2	713
7977-3703	0.02782	10.35	0.40	0.9	653
8155-6102	0.03081	10.36	0.35	1.7	1041
7977-3704	0.02724	10.36	-0.39	3.3	305
8655-9102	0.04505	10.42	0.28	0.8	330
8450-6102	0.04200	10.43	0.64	1.0	633
8616-9102	0.03039	10.44	0.65	3.2	823
8082-12701	0.02703	10.48	0.12	3.01	1038
8156-3701	0.05273	10.52	0.87	0.9	424
8081-3704	0.05400	10.56	0.96	2.0	222
8081-9101	0.02846	10.60	0.32	1.8	269
8077-6104	0.04601	10.73	0.65	1.3	876
8952-12701	0.02856	10.73	-0.38	1.61	63
8078-6103	0.02859	10.75	0.61	1.9	932
8616-12702	0.03083	10.76	-0.24	4.42	190
8616-6104	0.05426	10.77	0.26	0.8	348
7977-12705	0.02724	10.85	0.47	4.85	367
8086-9101	0.04003	10.94	0.12	6.0	375
8078-12701	0.02698	10.95	0.40	3.51	705
8241-3704	0.06617	11.00	1.21	1.9	561
8083-12702	0.02104	11.22	0.67	2.62	1893
7977-9101	0.02656	11.23	0.14	3.8	165
8623-6104	0.09704	11.28	1.18	3.7	276
8082-12704	0.13214	11.42	0.77	5.34	36

не с ребра!

Много областей HII!

Достаточно массивные; НЕ ВСЕ на главной последовательности

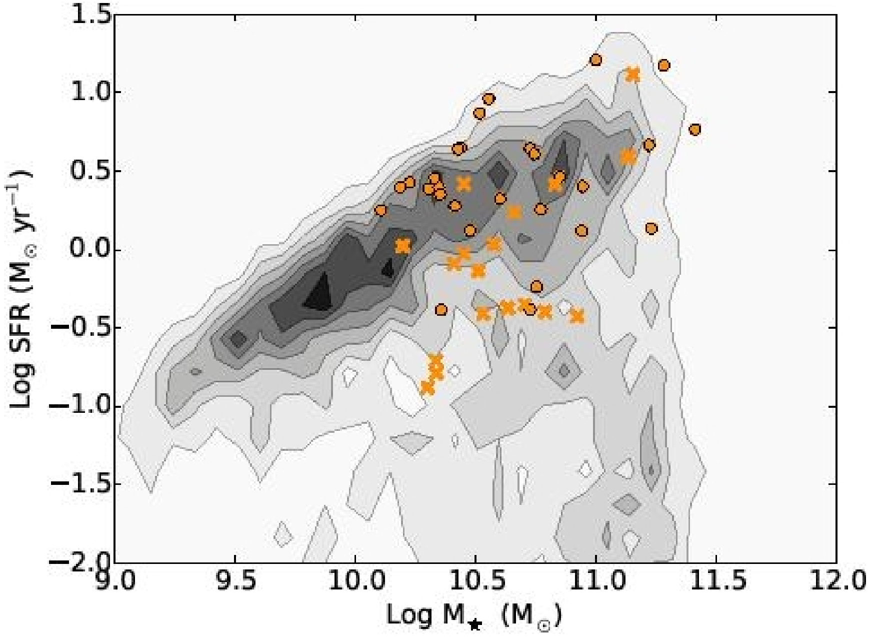

Figure 1. The global stellar mass and star formation rates for all of MaNGA DR15 (grey contours) and the ALMaQUEST sample (symbols). The 28 galaxies used in this study are shown as filled circles. ALMaQUEST sample galaxies excluded due to either high inclination or insufficent numbers of star forming spaxels are shown with crosses.

Три масштабирующих соотношения:

- Главная последовательность: плотность звездного компонента VS плотность темпов звездообразования.
- Закон Кенниката-Шмидта: плотность темпов звездообразования VS плотность молекулярного газа.
- Соотношение плотности газа и плотности звезд в данном месте.

Все 15000 спакселей…

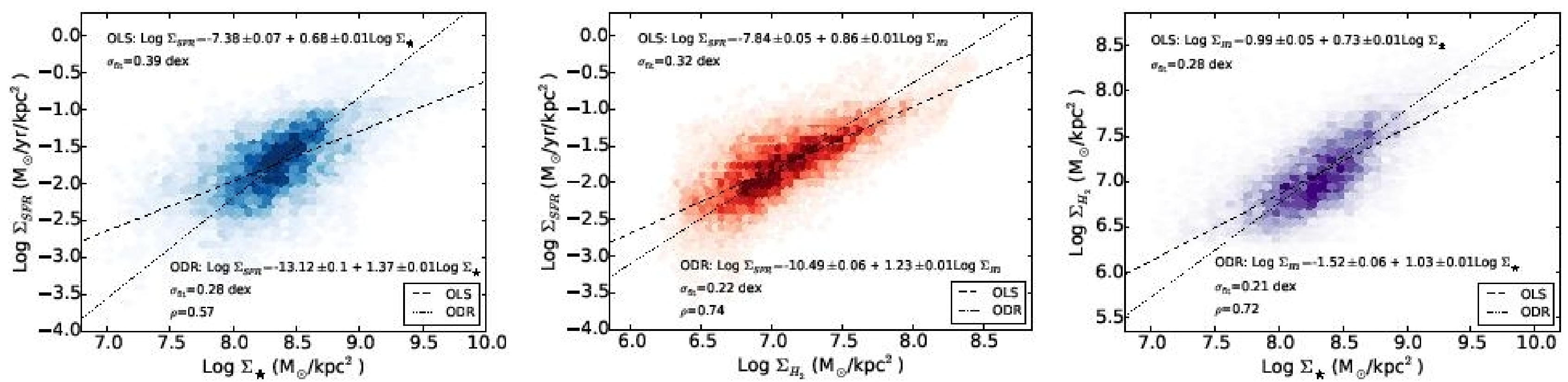

Figure 2. Ensemble star formation relations for 15,035 spaxels in our sample of ALMaQUEST 28 galaxies. Left panel: The resolved star-forming main sequence. Middle panel: the resolved Schmidt-Kennicutt relation. Right panel: The resolved molecular gas main sequence. The ordinary least squares and the orthogonal distance regression fits are shown by dashed and dotted lines respectively. The coefficients (and their errors) of the OLS and ODR fits are reported in the top and bottom each panel, along with the scatter around each best fit (σ_{fit}), as well as the Pearson correlation coefficient (ρ).

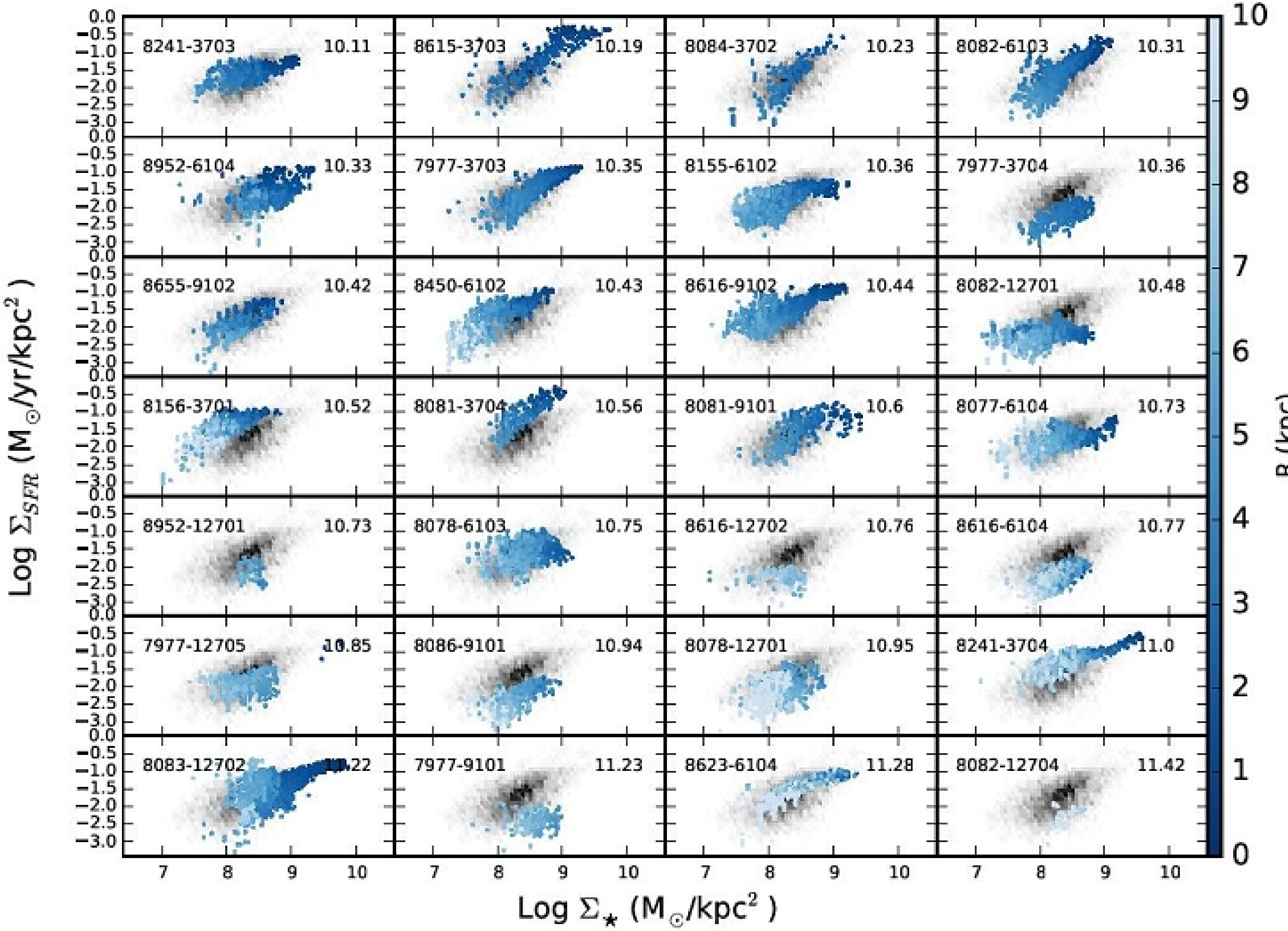

8241-3703
10.11
8615-3703
10.19
8084-3702
10.23
8082-6103
10.31
8952-6104
10.33
7977-3703
10.35
8155-6102
10.36
7977-3704
10.36
8655-9102
10.42
8450-6102
10.43
8616-9102
10.44
8082-12701
10.48
8156-3701
10.52
8081-3704
10.56
8081-9101
10.6
8077-6104
10.73
8952-12701
10.73
8078-6103
10.75
8616-12702
10.76
8616-6104
10.77
7977-12705
10.85
8086-9101
10.94
8078-12701
10.95
8241-3704
11.0
8083-12702
11.22
7977-9101
11.23
8623-6104
11.28
8082-12704
11.42
Log Σ_{SFR} (M$_\odot$/yr/kpc^2)
Log $\Sigma_\star$ (M$_\odot$/kpc^2)
R (kpc)

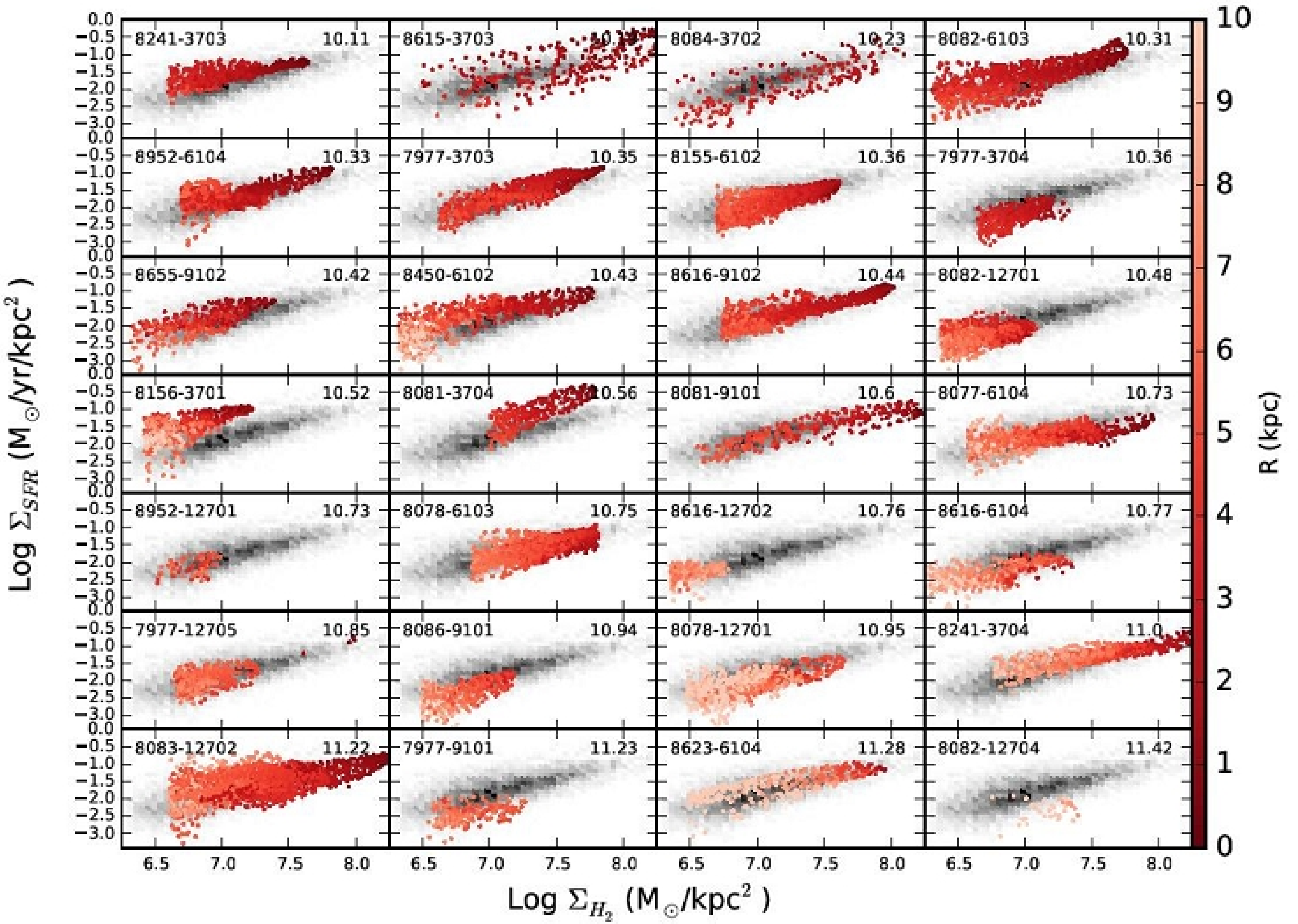

8241-3703 10.11
8615-3703 10.19
8084-3702 10.23
8082-6103 10.31
8952-6104 10.33
7977-3703 10.35
8155-6102 10.36
7977-3704 10.36
8655-9102 10.42
8450-6102 10.43
8616-9102 10.44
8082-12701 10.48
8156-3701 10.52
8081-3704 10.56
8081-9101 10.6
8077-6104 10.73
8952-12701 10.73
8078-6103 10.75
8616-12702 10.76
8616-6104 10.77
7977-12705 10.85
8086-9101 10.94
8078-12701 10.95
8241-3704 11.0
8083-12702 11.22
7977-9101 11.23
8623-6104 11.28
8082-12704 11.42
Log Σ_{SFR} (M$_\odot$/yr/kpc^2)
Log Σ_{H_2} (M$_\odot$/kpc^2)
R (kpc)

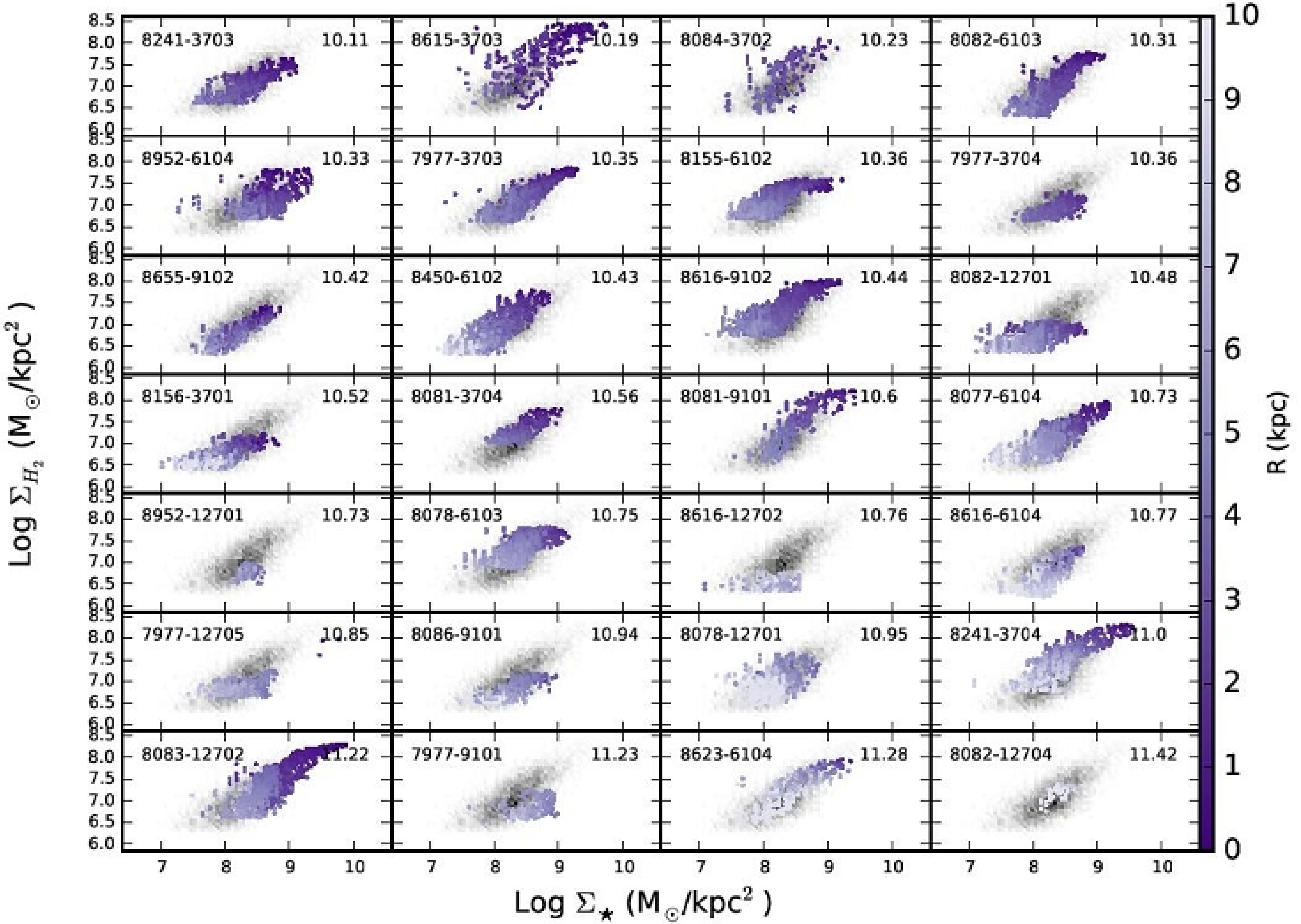

8241-3703 10.11
8615-3703 10.19
8084-3702 10.23
8082-6103 10.31
8952-6104 10.33
7977-3703 10.35
8155-6102 10.36
7977-3704 10.36
8655-9102 10.42
8450-6102 10.43
8616-9102 10.44
8082-12701 10.48
8156-3701 10.52
8081-3704 10.56
8081-9101 10.6
8077-6104 10.73
8952-12701 10.73
8078-6103 10.75
8616-12702 10.76
8616-6104 10.77
7977-12705 10.85
8086-9101 10.94
8078-12701 10.95
8241-3704 11.0
8083-12702 11.22
7977-9101 11.23
8623-6104 11.28
8082-12704 11.42
Log Σ_{H_2} (M$_\odot$/kpc^2)
Log $\Sigma_\star$ (M$_\odot$/kpc^2)
R (kpc)

Какое соотношение самое ‘тесное’?

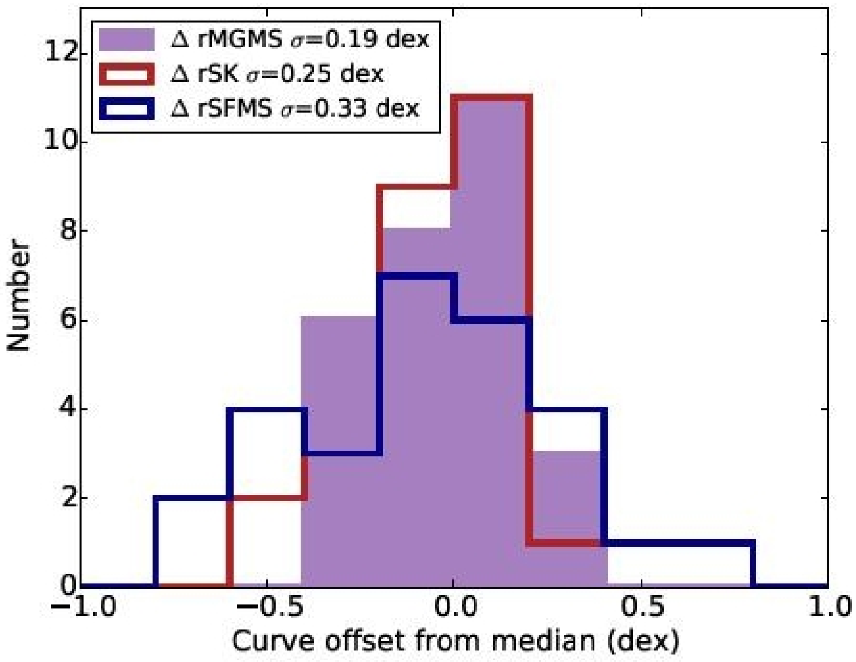

Figure 8. Histogram distribution of galaxy-by-galaxy offsets from the median scaling relations. Offsets from the median rSFMS, rSK relation and rMGMS are shown in blue, red and purple respectively. The galaxy-to-galaxy variation is greatest in the rSFMS and least in the rMGMS.

А какое ‘вытекает’ из двух других?

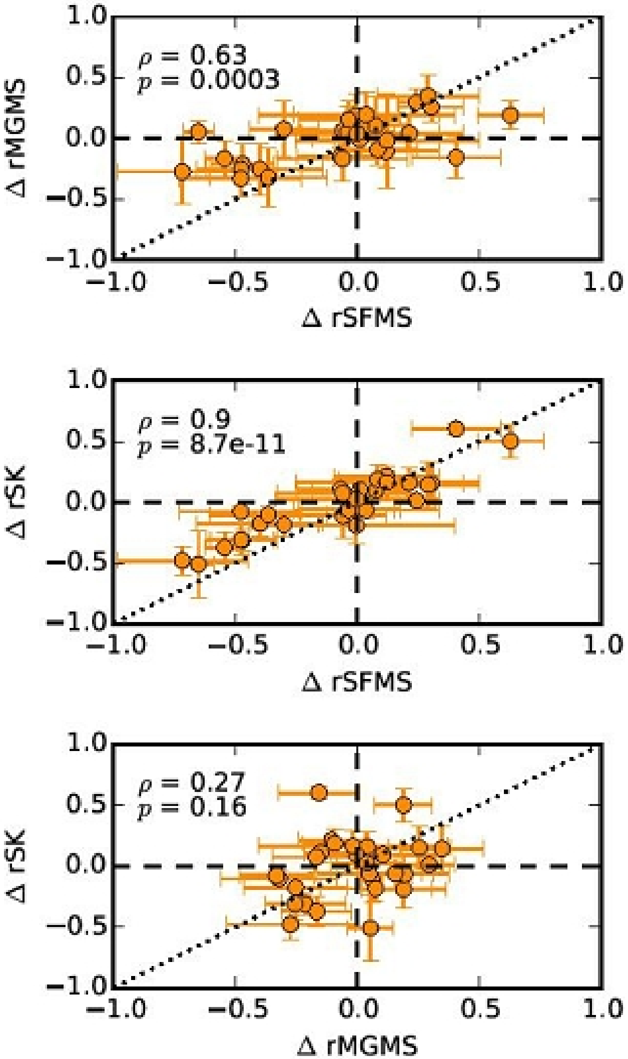

- Когда отклонения НЕ коррелируют – это означает, что под соотношениями лежит разная физика.
- А вот главная последовательность – есть следствие закона KS и зависимости доли молекулярного газа от локальной плотности звездного населения

Какие глобальные характеристики галактики управляют нуль-пунктами соотношений?

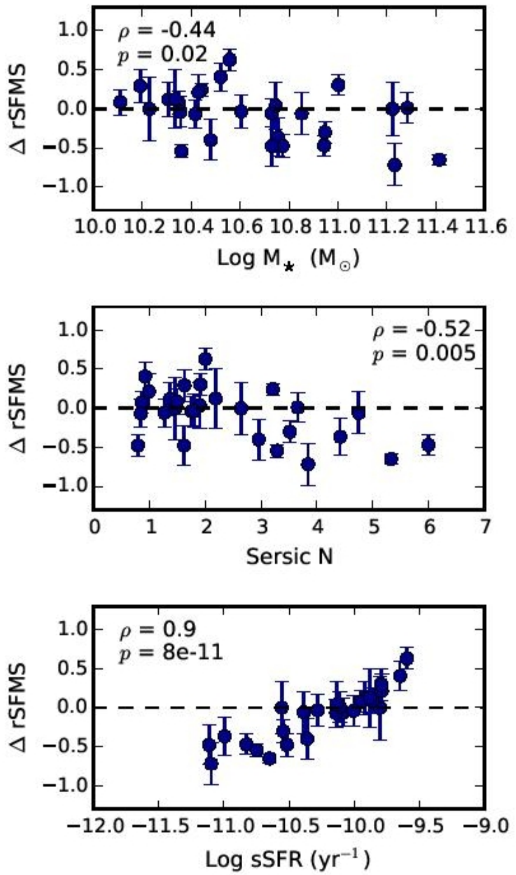

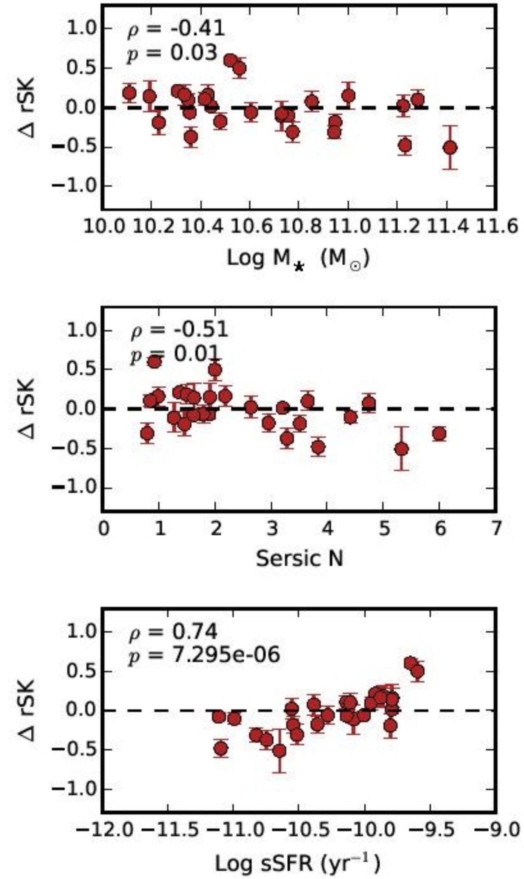

10. Galaxy-by-galaxy offset from the median rSFMS relation a

Какие глобальные характеристики галактики управляют нуль-пунктами соотношений?

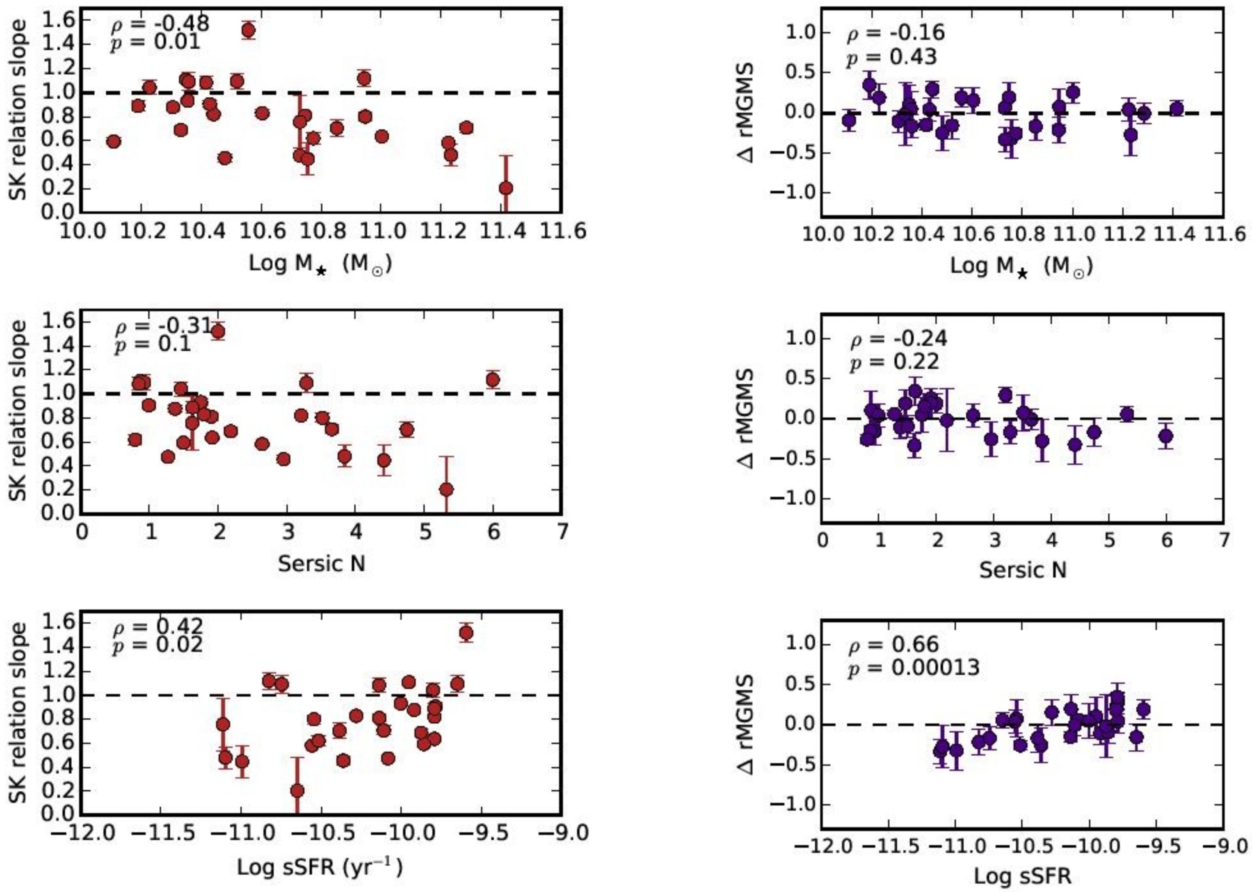

ну вот ОТЧАСТИ морфология...

ArXiv: 2012.04772

The ALMaQUEST Survey: VI. The molecular gas main sequence of 'retired' regions in galaxies.

Sara L. Ellison[1], Lihwai Lin[2], Mallory D. Thorp[1], Hsi-An Pan[3], Sebastian F. Sánchez[4], Asa F. L. Bluck[6], Francesco Belfiore[7]

[1] *Department of Physics & Astronomy, University of Victoria, Finnerty Road, Victoria, British Columbia, V8P 1A1, Canada*
[2] *Institute of Astronomy & Astrophysics, Academia Sinica, Taipei 10617, Taiwan*
[3] *Max-Planck-Institut für Astronomie, Königstuhl 17, D-69117 Heidelberg, Germany*
[4] *Instituto de Astronomía, Universidad Nacional Autonoma de Mexico, A. P. 70-264, C.P. 04510, Mexico, D.F., Mexico*
[6] *Kavli Institute for Cosmology & Cavendish Astrophysics, University of Cambridge, Madingley Road, Cambridge, CB3 0HA, UK*
[7] *INAF — Osservatorio Astrofisico di Arcetri, Largo E. Fermi 5, I-50125, Florence, Italy*

10 December 2020

ABSTRACT

In order to investigate the role of gas in the demise of star formation on kpc-scales, we compare the resolved molecular gas main sequence (rMGMS: Σ_{H_2} vs $\Sigma_\star$) of star-forming regions to the sequence of 'retired' regions that have ceased to form new stars. Using data from the ALMaQUEST survey, we find that retired spaxels form a rMGMS that is distinct from that of star-forming spaxels, offset to lower Σ_{H_2} at fixed $\Sigma_\star$ by a factor of ~5. We study the rMGMS of star-forming and retired spaxels on a galaxy-by-galaxy basis for eight individual ALMaQUEST galaxies. Six of these galaxies have their retired spaxels concentrated within the central few kpc. Molecular gas is detected in 40-100% of retired spaxels in the eight galaxies in our sample. Both the star-forming and retired rMGMS show a diversity in normalization from galaxy-to-galaxy. However, in any given galaxy, the rMGMS for retired regions is found

Параллельная последовательность?

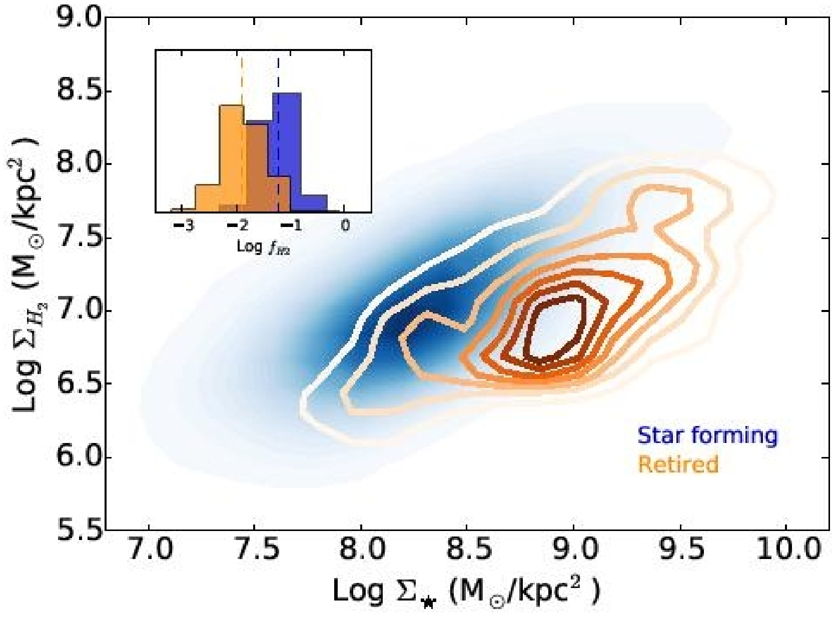

Figure 1. The resolved molecular gas main sequence for ~19,000 star forming spaxels (blue shading) and ~1,500 retired spaxels (orange contours) in the full ALMaQUEST sample (46 galaxies). Whereas the retired spaxels form their own version of a rMGMS, it is offset to lower Σ_{H_2} at fixed $\Sigma_\star$. The inset histogram shows the (normalized) distribution of molecular gas fractions of the two populations. The (logarithmic) median gas fractions (shown by vertical dashed lines) of the star forming and retired populations are −1.2 and −1.9 dex, respectively. The detection threshold for Σ_{H_2} varies from galaxy-to-galaxy, but is typically log Σ_{H_2} ~ 6.3 – 6.8 $M_\odot kpc^{-2}$.

А вот от галактики к галактике снова все сложно…

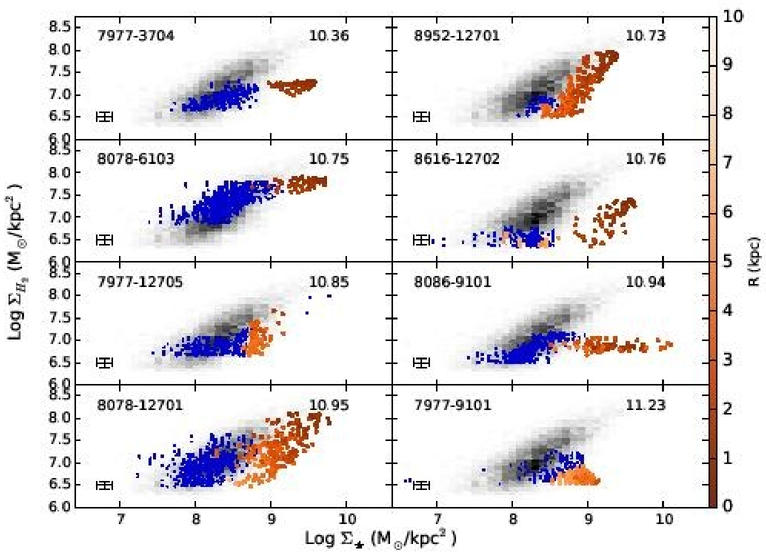

Figure 3. The rMGMS for eight ALMaQUEST galaxies. Star-forming spaxels are shown in blue and retired spaxels are shown in orange, with shading that indicates the distance from the centre of the galaxy in kpc. The MaNGA plate-ifu is given in the top left of each panel and the stellar mass in the top right. The retired spaxels show a distinct rMGMS compared with the star-forming spaxels in the same galaxy. Typical measurement uncertanties are shown in the lower left of each panel; these do not include systematic uncertainties or modelling assumptions , e.g. due to choice of α_{CO}, initial mass function, extinction law etc.

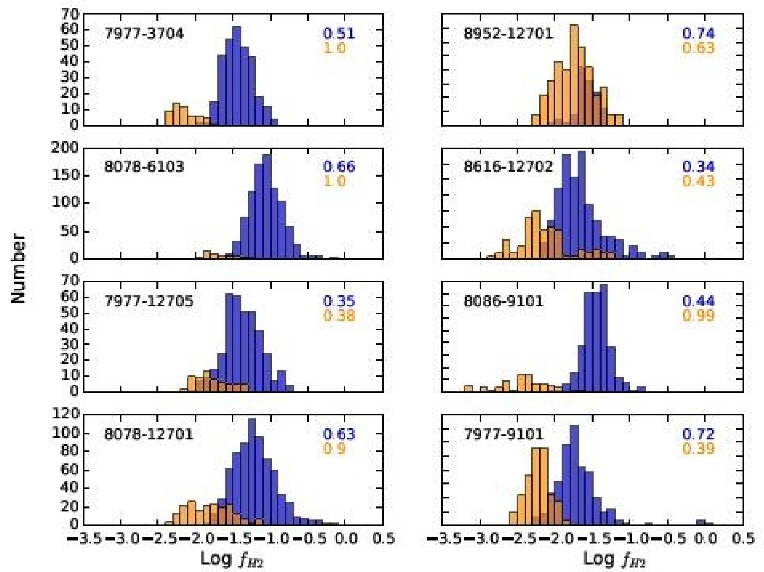

Figure 4. Gas fraction distributions for the eight galaxies in our sample. The distribution for star-forming spaxels is shown in blue and for retired spaxels in orange. The MaNGA plate-ifu is given in the top left of each panel and the fraction of star-forming/retired spaxels detected in CO (S/N>2) in the top right. Panels appear in the same order as Fig. 3. Retired spaxels have lower molecular gas fractions by up to an order of magnitude compared with star-forming spaxels in the same galaxy.